

1 **The role of albedo and accumulation in the 2010 melting record in Greenland.**

2
3 *M. Tedesco¹, X. Fettweis^{2,3}, M. R. van den Broeke³, R. S. W. van de Wal³, C. J. P. P.*
4 *Smeets³, W. J. van de Berg³, M.C. Serreze⁴ and, J. E. Box^{5,6}*

5
6 *1) The City College of New York, CUNY, New York, NY, USA*

7 *2) University of Liège, Liège, Belgium*

8 *3) Utrecht University, Institute for Marine and Atmospheric research Utrecht (IMAU) Utrecht University, Utrecht, The Netherlands*

9 *4) National Snow and Ice Data Center, Boulder, CO, USA*

10 *5) Department of Geography, The Ohio State University, Columbus Ohio, USA*

11 *6) Byrd Polar Research Center, Columbus Ohio State University, USA*

12
13 **Abstract**

14
15 *Analyses of remote sensing data, surface observations and output from a regional*
16 *atmosphere model point to new records in 2010 for surface melt and albedo, runoff, the*
17 *number of days when bare ice is exposed and surface mass balance of the Greenland ice*
18 *sheet, especially over its west and southwest regions. Early melt onset in spring,*
19 *triggered by above-normal near-surface air temperatures, contributed to accelerated*
20 *snowpack metamorphism and premature bare ice exposure, rapidly reducing the surface*
21 *albedo. Warm conditions persisted through summer, with the positive albedo feedback*
22 *mechanism being a major contributor to large negative surface mass balance anomalies.*
23 *Summer snowfall was below average. This helped to maintain low albedo through the*
24 *2010 melting season, which also lasted longer than usual.*

25

26 **1 Introduction and objectives**

27

28 Large positive near-surface temperature anomalies occurred along the coast of the
29 Greenland ice sheet during the year 2010 (*e.g.*, *Box et al.*, 2010). For example, at Aasiaat
30 (68°42'35"N 52°52'10"W), along Greenland's west coast, 2010 as a whole was the
31 warmest since records began in 1951, with records also set for winter, spring, May and
32 June. Narsarssuaq (61°09'39"N 45°25'32"W), in southern Greenland, saw its warmest
33 winter and spring, its warmest May, and its warmest annual average since records began
34 in 1951; Nuuk, the capital of Greenland, located along the southwest coast (64°10'30"N,
35 51°44'20"W), with a temperature time series extending back to 1873, saw record warmth
36 for winter, spring, summer and the year as a whole (*Cappelen*, 2010).

37 Surface melting over the Greenland ice sheet, which can be estimated from satellite
38 data, ground observations or models (*Abdalati and Steffen*, 1997, *Mote*, 2007, *Nghiem et*
39 *al.*, 2001, *Hall et al.*, 2009, *Tedesco*, 2007, *Hanna et al.*, 2008, *Fettweis et al.*, 2010b,
40 *Ettema et al.*, 2010) was also exceptional in 2010 (*Box et al.*, 2010). Results obtained
41 applying the algorithm reported in *Tedesco* (2007) to spaceborne microwave brightness
42 temperatures (*e.g.*, *Armstrong et al.*, 1994, *Knowles et al.*, 2002) are consistent with those
43 reported in *Box et al.* (2010), showing that large areas of the ablation zone in south
44 Greenland underwent melting up to 50 days longer in 2010 compared to the 1979 – 2009
45 average, with melting in 2010 starting exceptionally early at the end of April and ending
46 quite late in mid September (Figure 1). These results are confirmed by surface
47 measurements.

48

49 Near-surface air temperature is often used as a proxy for surface melting. Previous
50 studies have analyzed exceptional melting events mainly focusing on the relationship
51 between melt and near surface temperatures (*e.g.*, *Mote 2007, Tedesco 2007*). However,
52 melting and, consequently the surface mass balance (SMB), also depend on
53 accumulation, radiation conditions, refreezing and sublimation, the latter relatively small
54 and constant in time (*Box and Steffen, 2001; Fettweis, 2007; Van den Broeke et al.,*
55 *2008*). Surface melt and albedo are intimately linked: as melting increases, so does snow
56 grain size, leading to a decrease in surface albedo which then fosters further melt. Also,
57 changes in accumulation can affect the seasonal evolution of surface albedo, that
58 influences the SMB. It is hence not sufficient to analyze near-surface temperature trends
59 to understand the driving mechanisms of extreme mass loss and studying the role of
60 albedo and accumulation becomes crucial to provide a more robust understanding of the
61 exceptional melting detected by satellite microwave sensors.

62

63 In this study, we report results derived from spaceborne sensors, surface glaciological
64 observations and regional atmospheric model outputs regarding the surface albedo,
65 accumulation and bare ice exposure over the Greenland ice sheet during the summer of
66 2010. Our results indicate that negative surface albedo anomalies were especially
67 prominent over west Greenland, with bare ice exposed earlier than previous years. In
68 addition, increased runoff and reduced accumulation likely contributed to a strongly
69 negative SMB.

70

71 **2 Data and methodologies**

72 2.1 Satellite data

73 We use the Moderate-resolution Imaging Spectroradiometer (MODIS) 16-day gridded
74 albedo product (<http://www-modis.bu.edu/brdf/userguide/intro.html>) to study anomalies
75 in both directional hemispherical reflectance (black-sky albedo) and bi-hemispherical
76 reflectance (white-sky albedo) in the shortwave, visible and near-infrared bands. Black-
77 sky albedo is the albedo under direct illumination (or direct beam contribution) where the
78 white-sky albedo is the one under diffuse or indirect light. Black- and white-sky albedos
79 can be combined as a function of the diffuse skylight for a representation of the actual
80 albedo such as measured by field instruments (*Lucht et al., 2000*). The MODIS product,
81 which has been evaluated over Greenland (e.g. *Stroeve et al., 2005*), is provided every 8
82 days using 16 days acquisitions from both the TERRA and AQUA satellites. Data are
83 provided on a 0.05° latitude/longitude grid. While we discuss only for the shortwave
84 white sky albedo, conclusions that follow also apply to black-sky, visible and near
85 infrared albedos.

86 2.2 Glaciological data

87 The Institute of Marine and Atmospheric Research Utrecht, (IMAU) installed several
88 Automatic Weather Stations (AWSs) along the Kangerlussuaq transect (K-transect, 67°N)
89 in southwest Greenland in August 2003, located at increasing distance from the ice sheet
90 margin and increasing elevations, up to 1500 m a.s.l. (*van den Broeke et al., 2008*). This
91 part of Greenland is characterized by a 100 km wide ablation zone and an average
92 equilibrium line altitude (ELA) of approximately 1500 m a.s.l. The stations are equipped
93 with radiation sensors. SMB balance can be estimated at the local spatial scale from
94 stakes and acoustic height rangars. Apart from atmospheric radiation, the stations

95 measure basic meteorological variables like wind speed and direction, temperature,
96 relative humidity and air pressure. Surface mass-balance measurements are performed
97 along the K-transect at selected sites. The three AWS sites (S5, S6 and S9) are located,
98 respectively, 6 km (S5), 37 km (S6) and 91 km (S9) from the ice sheet margin at an
99 elevation of 490 m (S5), 1020 m (S6) and 1520 m (S9) a.s.l. Mass-balance sites (S4,
100 SHR, S7,S8,S10) are located 3km (S4), 14 km (SHR), 52 km (S7), 63 km (S8) and 143
101 km (S10) from the ice sheet margin at an elevation of 340/390 m (S4, 340 m was the
102 initial value), 710 m (SHR), 1110 m (S7), 1260 m (S8) and 1850 m (S10) a.s.l. Mass
103 balance data are available over the period 1991-2010. Weather station data are available
104 for the period 2003-2010. Further information on the stations can be found in *Van de Wal*
105 *et al. (2005)*.

106 *2.3 The Surface and Energy balance Model.*

107 The surface and energy balance model is the regional climate model MAR (Modèle
108 Atmosphérique Régional), coupled to the 1-D Surface Vegetation Atmosphere Transfer
109 scheme SISVAT (Soil Ice Snow Vegetation Atmosphere Transfer). The schemes and the
110 set-up employed for the present study are fully described in *Fettweis et al. (2010a)*,
111 *Fettweis (2007)* and *Lefebvre et al. (2005)*. Differently from most existing models, MAR
112 is coupled to a snow physical model called CROCUS (*Brun et al., 1992*). CROCUS is a
113 one-dimensional multi-layered energy balance model consisting of a thermodynamic
114 module, a water balance module taking into account the refreezing of meltwater, a snow
115 metamorphism module, a snow/ice discretization module and an integrated surface
116 albedo module. For this study, MAR outputs are derived at a spatial resolution of 25 km
117 for the period 1958 - 2010. The ERA-40 reanalysis (1957–2001), the ERA-INTERIM

118 reanalysis (2002- June 2010) and after that, the operational analysis (Jul 2010 - Sep 2010)
119 from ECMWF are used to initialize the meteorological fields at the beginning of the
120 simulation in September 1957 and to force every 6 hours the lateral boundaries with
121 temperature, specific humidity and wind components during the simulation. The Sea
122 Surface Temperatures (SST) and the sea-ice extent in the SISVAT module are also
123 prescribed by the reanalyses. No re-initialization or correction are applied to the model
124 outputs. The (re)analysis data are available every 6 h at a resolution of at least one degree
125 .The MAR spatial domain is represented by an area of 2000 km x 3500 km centered at
126 70°N latitude and 40°W longitude. There are at least 10 pixels between the Greenland and
127 the model boundaries. The integration domain is shown in *Fettweis et al. (2005)*. An ice
128 sheet mask is then applied to analyze only those pixels belonging to the ice sheet
129 (*Fettweis, 2008*). Outputs from the MAR model have been shown to be consistent with
130 results obtained from passive microwave observations (*Fettweis et al., 2010b*).

131

132 **2 Results and discussion.**

133

134 Figure 2a shows the MODIS shortwave white-sky albedo anomaly for the months of
135 May through August (MJJA), relative to the 2004 – 2009 mean. This period was chosen
136 because ground albedo measurements for comparison are available starting in 2004. The
137 MODIS record itself spans a longer period, 2001-2009. The strong negative albedo
138 anomalies along the southwest margin of the ice sheet (more than -0.10) are consistent
139 with the positive melting anomalies detected by the microwave sensors and simulated by
140 the MAR model (see Figure 1). As assessed using the complete MODIS record, the
141 shortwave 2010 albedo averaged over MJJA was up to 0.15 below the mean over

142 southwest Greenland, with the largest negative anomalies during August. August albedo
143 anomalies are as large as -0.25 near the Nuuk area and -0.2 along most of the
144 southwestern regions of the Greenland Ice Sheet. The observed 2010 albedo anomalies
145 can be the consequence of: 1) a reduced frequency and/or amount of snowfall; 2)
146 enhanced melting; 3) exposure of bare ice for a longer period of time during the melting
147 season. Figure 2b provides the standardized anomaly map (the departure from the mean
148 divided by the standard deviation of the distribution) of the number of days when bare ice
149 was exposed in 2010 based on MAR outputs. According to MAR, in 2010 bare ice was
150 exposed for a period up to four times longer than the standard deviation computed over
151 the 1979 – 2009 period along the western region of the ice sheet, with absolute anomalies
152 peaking up to 50 days. Figure 2c shows the summer snowfall anomalies (in mm water
153 equivalent, WE) from MAR, still relative to 1979 – 2009 means. The model suggests that
154 summer accumulation in 2010 over the southwestern part of the Greenland ice sheet was
155 two standard deviations below the 1979 – 2009 mean. This, together with large positive
156 near-surface temperature anomalies, very likely led to the premature exposure of bare ice
157 (Figure 2b) and the reduced albedo (Figure 2a).

158

159 Figure 3a summarizes MAR estimates and measurements on the ice of SMB (mWE)
160 averaged over four IMAU AWSs (SHR, S6, S8 and S9). Data from the AWSs indicate
161 that average SMB values in 2010 were 2.3 standard deviations below the 1991 – 2010
162 average (the record from the stations begin in 1991). Moreover, according to MAR,
163 average SMB values in 2010 at the IMAU stations locations were 2.3 standard deviations
164 below the average over the same period. For both measured and modeled quantities, the

165 SMB in 2010 was the lowest for the data record. As an example, Figure 3b shows the
166 time series of MODIS and IMAU surface albedos for 2010 together with the 2004 – 2009
167 average values at the S9 station (67°03'02" N 48°13'53" W, 1500 m a.s.l.). Differences in
168 absolute values from the satellite and ground observations reflect the spatial scale at
169 which MODIS data are collected or re-gridded, atmospheric corrections, and the MODIS
170 albedo retrieval algorithm. The figure highlights that both MODIS and the station data
171 show a decline in albedo through the 2010 melting season, with the absence of sporadic
172 peaks that would result from snowfall events (which are present during years when
173 positive anomalies of summer snowfall are measured and modeled). The match between
174 the seasonal trends derived from MODIS and those measured on the ice lends credence to
175 the MAR results, pointing to negative snowfall anomalies for 2010 (Figure 2c) and
176 premature exposure of bare ice (Figure 2b).

177 Early exposure of bare ice and reduced snowfall in 2010 are also evident from surface
178 height measurements along the K-transect. Figure 3c illustrates surface height changes
179 over the years 2003 through 2010 at the S9 station. We focus on the station S9 as it is
180 situated at 1500 m elevation, at the approximate ELA, where annual accumulation should
181 on average equal ablation. From Figure 3c, the net annual surface height change for the
182 years 2004, 2007 and 2008 is close to 0 m (indicating that the position of the ELA was
183 close to the station elevation), contrasting with the years of 2005 and 2006 when the net
184 surface height change was $\sim 0.3 - 0.4$ m (indicating that the station was above the ELA
185 for those years). Reduced accumulation and exceptionally large ablation during 2010 are
186 evident. The surface height data clearly indicate that accumulation for 2010 at the S9
187 station was only about 0.6 m (vs. the 2003 – 2009 average of ~ 1.05 m) and the surface

188 height value recorded at the end of August was -0.7 m (vs. the 2003 – 2009 average of ~ -
189 0.05 m), below any value previously recorded. The total change in surface height was ~
190 1.3 m, the highest loss over the past twenty years. The extreme nature of the SMB loss in
191 2010 is also evident at the other stations along the K-transect (not shown here).

192

193 The MAR allows us to examine conditions back to 1958, placing 2010 in the context
194 of a longer time series. According to MAR, the hydrological year (October through
195 September) 2009-2010 SMB anomaly set a new record low of -310 Gt, 2.6 standard
196 deviations below the 1958-2009 average, surpassing the previous record of 2.3 standard
197 deviations set in 2007. Snowfall for the period October 1st 2009 – September 30th 2010
198 was about 68 Gt (1.5 standard deviations below average) and runoff was 243 Gt, or 2.4
199 standard deviations above the 1958-2009 average. Figure 4 shows monthly standardized
200 anomalies for 2010 (using 1979 – 2009 as a reference for consistency with the passive
201 microwave data time series) from MAR of near-surface temperature, albedo, snowfall,
202 meltwater, bare ice area and melt area excluding bare ice. Snowfall and near-surface
203 temperature anomalies for the autumn and winter of 2009 (September through April) are
204 also reported as a reference. The model indicates that surface albedo was persistently
205 below the average (2 standard deviations) for the summer. The meltwater produced in
206 May (August) was ~3 (~2.5) standard deviations above the mean. Bare ice area in May
207 was ~ 3.5 standard deviations above the mean and it remained persistently around 2
208 standard deviations above average through summer. By contrast, the melt area excluding
209 bare ice was exceptional in May, August and September.

210

211 **3 Conclusions**
212

213 Our analysis of remote sensing data, surface glaciological observations and model
214 outputs paints a portrait of strongly negative surface mass balance during 2010 promoted
215 by a strong warmth and enhanced by large negative anomalies of albedo and
216 accumulation and large positive anomalies of days when bare ice was exposed. Our
217 results clearly indicate that, beside near-surface temperature, other factors must be
218 considered to properly analyze extreme events such as the one that occurred in 2010. The
219 melt season started in mid April, after a warm and dry winter. Early melt onset, triggered
220 by large positive near-surface temperature anomalies during May 2010 (up to +4°C above
221 the mean) contributed to accelerated snowpack metamorphism and premature bare ice
222 exposure, with the consequence of rapidly reducing the surface albedo. Reduced
223 accumulation in 2010, and the positive albedo feedback mechanism are likely responsible
224 for the premature exposure of bare ice. While June and July temperature anomalies were
225 not exceptional, being +1.5°C above the 1979 – 2009 average, anomalously warm
226 conditions persisted with the positive albedo feedback mechanism contributing to large
227 negative SMB anomalies. Summer snowfall, which helps to increase surface albedo, was
228 below average. Melt during August and September was also exceptional, consistent with
229 low surface albedos and near surface temperature anomalies of up to +3°C, yielding a
230 long ablation season.

231 The surface melt time series from the combined passive microwave record, 1979-
232 present, is characterized by an upward trend, with considerable year-to-year variability
233 primarily related to atmospheric conditions. Viewed in this context, the unusually warm
234 conditions over the Greenland ice sheet in 2010 and reduced snowfall, can be related to

235 persistence of a 500 hPa high ridge from late spring through summer. Averaged for May
236 through August, 500 hPa heights were above normal over all of Greenland, with the
237 largest anomalies of up to 80 m over the south-central ice sheet. This anomalous ridge
238 was associated with 700 hPa temperature anomalies over south-central Greenland of up
239 to +3°C. The ridge and associated 700 hPa temperature anomaly was best expressed in
240 May and August, coinciding with near-surface air temperature records.

241

242 **Acknowledgments**

243

244 This work was supported by NSF grants ANS 0909388 and ARC 0901962, the NASA
245 Cryosphere Program, and the Ohio State University Climate Water and Carbon
246 Program. Field work along the K-transect has been supported by NWO/ALW.

247

248 **References**

249

250 Abdalati W and K Steffen 1997 Snowmelt on the Greenland Ice Sheet as Derived from
251 Passive Microwave Satellite Data *J. Climate* **10** 165-175

252 Armstrong R L, Knowles K W, Brodzik M J and Hardman M A 1994 updated 2009
253 *DMSP SSM/I Pathfinder Daily EASE-Grid Brightness Temperatures Boulder*

254 Colorado USA: National Snow and Ice Data Center, digital media

255 Box J E and Steffen K 2001 Sublimation estimates for the Greenland ice sheet using
256 automated weather station observations *J. Geophys. Res.* **106(D24)** 33965-33982

257 Box J E, Cappelen J, Decker D, Fettweis X, Mote T, Tedesco M and van de Wal R S W

258 2010, Greenland [in Arctic Report Card 2010],
259 <http://www.arctic.noaa.gov/reportcard>
260 Brun E, David P, Sudul M and Brunot G 1992, A numerical model to simulate
261 snowcover stratigraphy for operational avalanche forecasting *J. Glaciology* **38** 13–22
262 Cappelen J 2010 DMI Monthly Climate Data Collection 1768-2009, Denmark, The Faroe
263 Islands and Greenland *Dansk Meteorologisk Institut Technical report No. 10-05*
264 Ettema J, van den Broeke M R, van Meijgaard E, van de Berg W J, Box J E and Steffen
265 K 2010, Climate of the Greenland ice sheet using a high-resolution climate model –
266 Part 1: Evaluation *The Cryosphere Discussion* **4** 561-602 doi:10.5194/tcd-4-561-
267 2010
268 Fettweis X, Gallee H, Lefebvre L and van Ypersele J P 2005 Greenland surface mass
269 balance simulated by a regional climate model and comparison with satellite derived
270 data in 1990 – 1991, *Clim. Dyn.*, **24**, 623 – 640, doi:10.1007/s00382-005-0010-y.
271 Fettweis X. 2007 Reconstruction of the 1979-2006 Greenland ice sheet surface mass
272 balance using the regional climate model MAR, *The Cryosphere* **1** 21-40
273 Fettweis X. 2008 Impact of ice sheet mask and resolution on estimating the surface mass
274 balance of the Greenland ice sheet, *Proceedings of the European Geophysical Union*
275 *General Assembly*, Vienna, Austria, April 13 – 18, 2008, available at
276 <http://orbi.ulg.ac.be/bitstream/2268/36752/1/Fettweis-2008-EGU-Poster2.pdf>
277 Fettweis X, Mabilille G, Ericum M, Nicolay S and van den Broeke M 2010a The 1958-
278 2009 Greenland ice sheet surface melt and the mid-tropospheric atmospheric
279 circulation *Clim. Dynamycs* doi: 10.1007/s00382-010-0772-8
280 Fettweis X, Tedesco M, van den Broeke M and Ettema J 2010b, Melting trends over the

281 Greenland ice sheet (1958-2009) from spaceborne microwave data and regional
282 climate models *The Cryosphere Discussion* **4** 2433-2473

283 Hall D K, Nghiem S V, Schaaf C B, DiGirolamo N E and Neumann G 2009 Evaluation
284 of surface and near-surface melt characteristics on the Greenland ice sheet using
285 MODIS and QuikSCAT data *Journal of Geophysical Research - Earth Surface* **114**
286 F04006, doi:10.1029/2009JF001287

287 Hanna E, Huybrechts P, Steffen K, Cappelen J, Huff R, Shuman C, Irvine-Fynn T, Wise
288 S and Griffiths M 2008 Increased runoff from melt from the Greenland Ice Sheet: a
289 response to global warming, *J. Climate*, **21**, 331—341

290 Knowles K W, Ein G, Njoku E, Armstrong R L and Brodzik M J 2002 Nimbus-7 SMMR
291 Pathfinder Daily EASE-Grid Brightness Temperatures, Boulder, Colorado USA:
292 *National Snow and Ice Data Center, digital media*

293 Lefebre F, Fettweis X, Gallée H, van Ypersele J, Marbaix P, Greuell W and Calanca P
294 2005 Evaluation of a high-resolution regional climate simulation over Greenland
295 *Clim. Dynamycs* **25** 99-116 doi:10.1007/s00382-005-0005-8

296 Lucht W, Schaaf C B and Strahler A H 2000 An Algorithm for the Retrieval of Albedo
297 from Space Using Semiempirical BRDF Models *IEEE Trans. Geosci. Remote Sens.*
298 **38(2)** 977– 998

299 Mote T L 2007 Greenland surface melt trends 1973–2007: Evidence of a large increase in
300 2007 *Geophys. Res. Lett.* **34** L22507 doi:10.1029/2007GL031976.

301 Nghiem S V, Steffen K, Kwok R and Tsai w Y 2001 Detection of snowmelt regions on
302 the Greenland ice sheet using diurnal backscatter change *Journal of Glaciology* **47**
303 159, 539 - 547

304 Stroeve J C, Box J, Gao F, Liang S, Nolin A and Schaaf C 2005, Accuracy assessment of
305 the MODIS 16-albedo product for snow: Comparison with Greenland in situ
306 measurements *Rem. Sens. Env.* **94** 46-60 doi:10.1016/j.rse.2004.09.001
307 Tedesco M 2007 Snowmelt detection over the Greenland ice sheet from SSM/I brightness
308 temperature daily variations *Geophys. Res. Lett.* **34** L02504
309 doi:10.1029/2006GL028466.
310 Van de Wal R S W, Greuell W, Van den Broeke M, Reijmer C H and Oerlemans J 2005
311 Surface mass-balance observations and automatic weather station data along a
312 transect near Kangerlussuaq, West Greenland *Ann. Glaciol.* **42** 311-316
313 Van den Broeke M R, Smeets C J P P, Ettema J, van der Veen C, van de Wal R S W and
314 Oerlemans J 2008, Partitioning of energy and meltwater fluxes in the ablation zone
315 of the west Greenland ice sheet *The Cryosphere* **2** 179-189.

316

317 **Figure Captions**

318

319 Figure 1 a) anomaly map of melting days for 2010 derived from passive microwave
320 data. Hatched regions indicate where MAR-simulated meltwater production exceeds the
321 mean by at least two standard deviations; b) time series of the daily melt extent for the
322 2010 season, the 1979 – 2009 average and the year 2007; c) standardized melting index
323 (the number of melting days times area subject to melting) for 2010 from passive
324 microwave data over the whole ice sheet and for different elevation bands.

325 Figure 2. a) MODIS shortwave white sky albedo anomalies for 2010, relative to 2004
326 – 2009 means for May through August; b) MAR estimated standardized anomalies

327 (relative to 1979 – 2009) of the number of days with bare ice exposed for the period May
328 through September; c) May through September snowfall anomalies from MAR, relative
329 to 1979 – 2009 means.

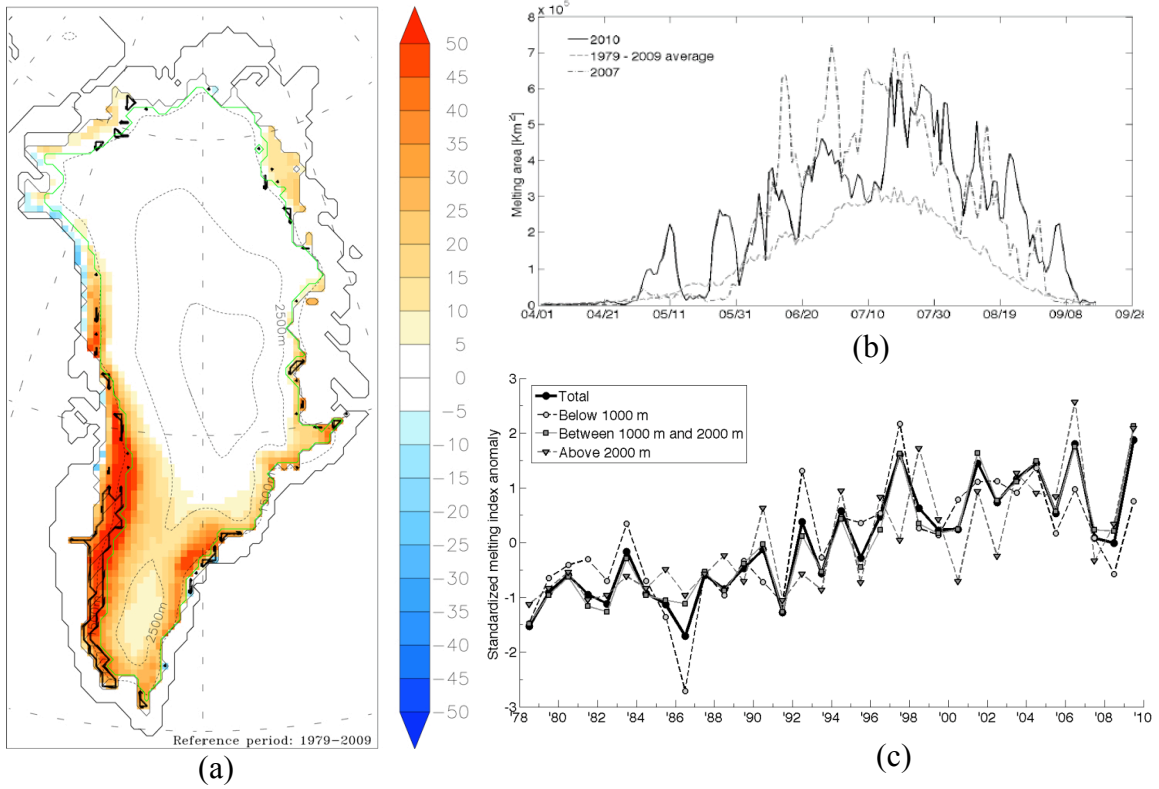
330 Figure 3. a) SMB from MAR and from sonic height ranger data (K-transect) for 1991-
331 2009 averaged over the S9, S8, S6 and SHR stations; b) time series of MODIS shortwave
332 albedo (black lines with circles) and albedo at the IMAU sites (gray lines with squares)
333 for 2010 at the S9 station. Dotted lines indicate averages for 2004 – 2009; c) data from
334 the sonic height ranger collected every half an hour over the last 7 years (September 2003
335 through September 2010) at the S9 station.

336 Figure 4. Monthly standardized anomalies for 2010 (relative to 1979 – 2009) for near-
337 surface temperature, albedo, snowfall, meltwater, bare ice area and melt area excluding
338 bare ice simulated by MAR.

339

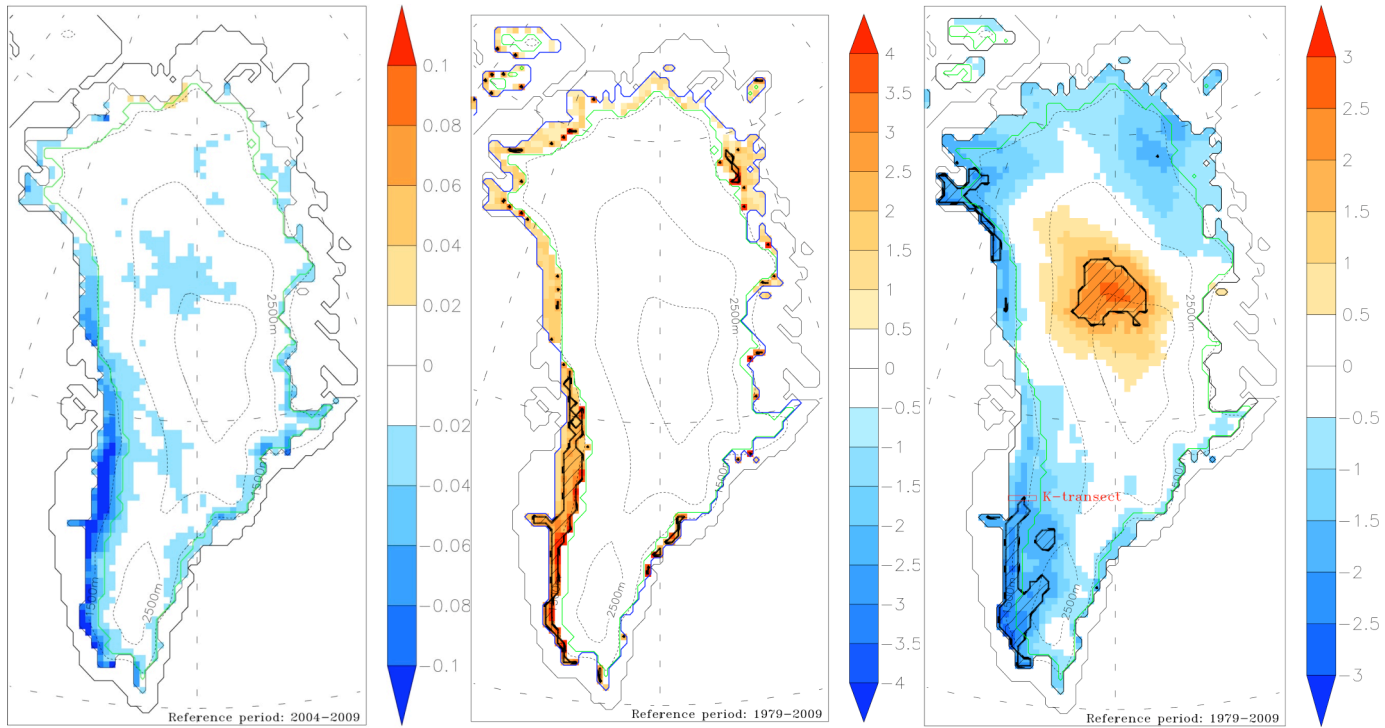
340

340
341



342
343
344
345
346

Figure 1.



2010 MODIS albedo anomaly

Normalized 2010 anomaly of the number of JJA days with bare ice

Normalized 2010 summer snowfall anomaly

(a)

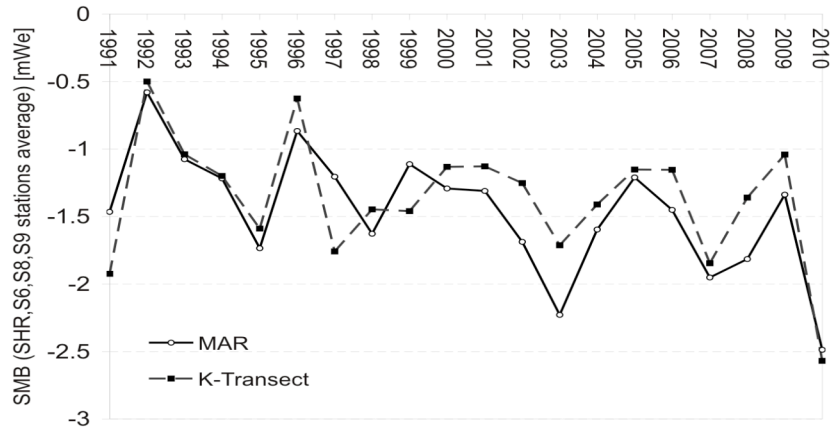
(b)

(c)

347
348
349
350
351
352
353

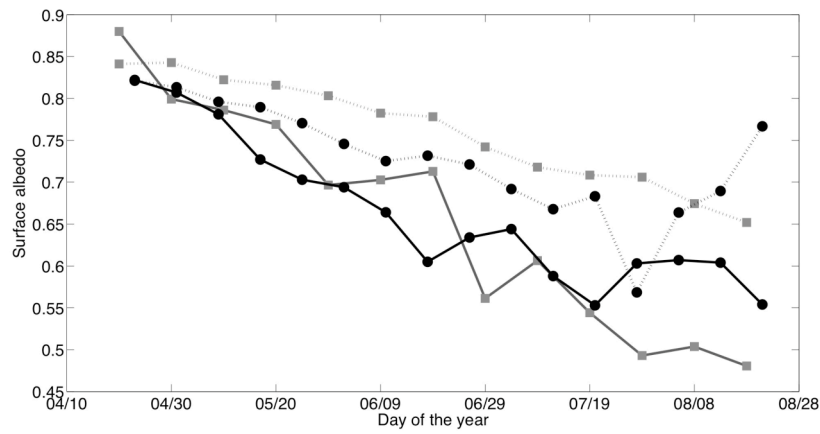
Figure 2.

354
355



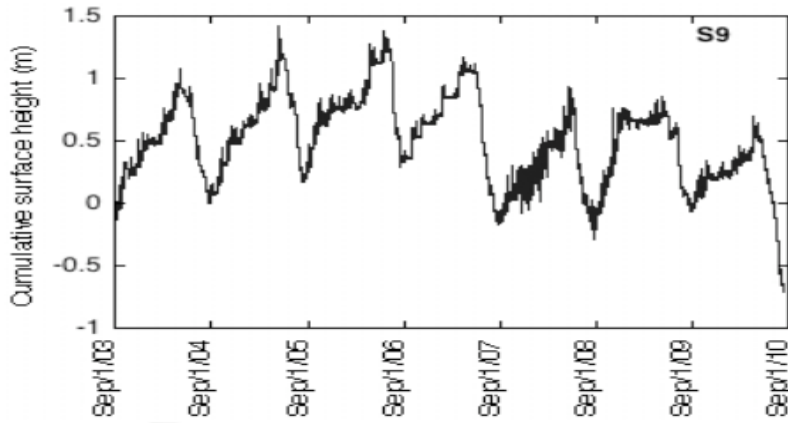
356
357

(a)



358
359

(b)

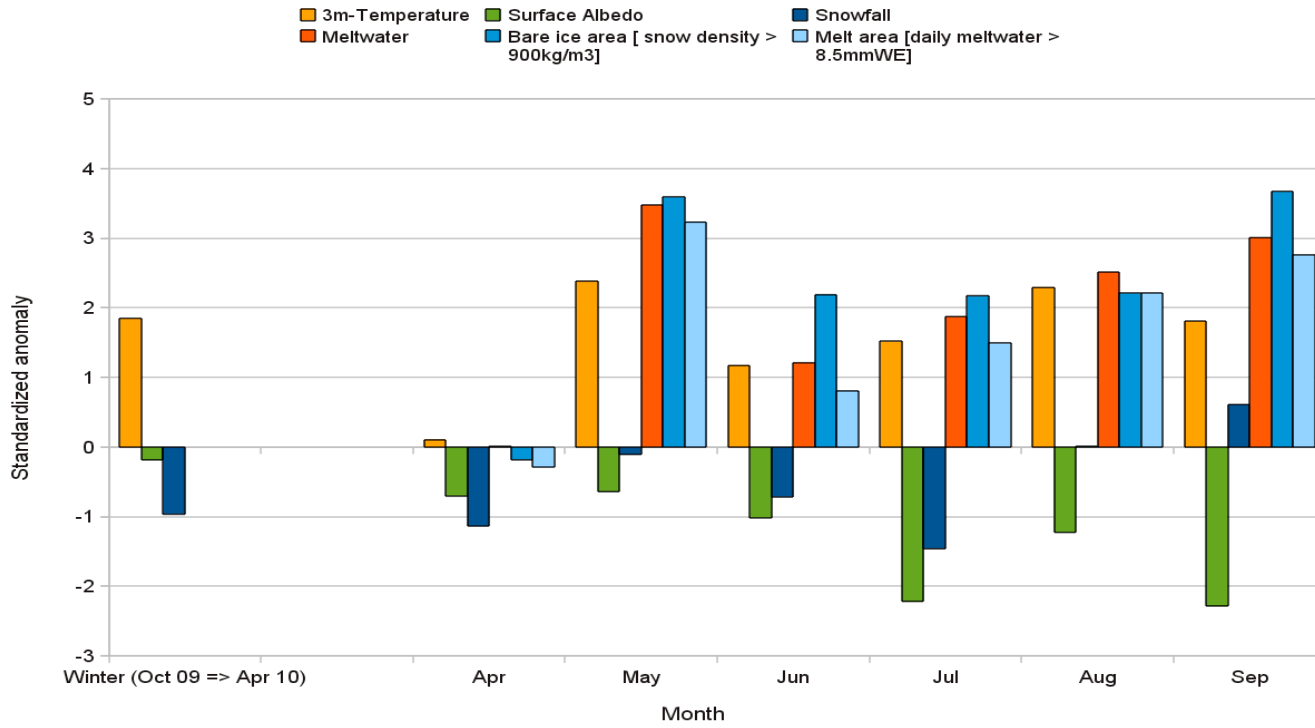


360
361
362

(c)

Figure .3

363



364
365
366
367

Figure 4.